miR-200b upregulation promotes migration of BEAS-2B cells following long-term exposure to cigarette smoke by targeting ETS1

JIN WANG[1*], RUIXIN YAO[1*], QIULIN LUO[1], LIRONG TAN[1], BEIBEI JIA[1], NAN OUYANG[1], YEZHOU LI[2], JIAN TONG[1] and JIANXIANG LI[1]

[1]Department of Toxicology, School of Public Health, Medical College of Soochow University, Suzhou, Jiangsu 215123, P.R. China; [2]School of Medicine, University of Manchester, M13 9PL Manchester, UK

Received January 13, 2021; Accepted May 18, 2021

DOI: 10.3892/mmr.2021.12201

Abstract. Cigarette smoking is the leading cause of all histological types of lung cancer, and the role that microRNAs (miRNAs) serve in its pathogenesis is being increasingly recognized. The aim of the present study was to investigate the role of miR-200b on migration in cigarette smoke-induced malignant transformed cells. In the present study, miR-200b expression was found to be increased in cigarette smoke (CS)-exposed BEAS-2B cells, lung cancer cell lines and tumor tissue samples. Using wound healing and Transwell migration assays, the migratory ability was shown to be increased in miR-200b-overexpressing cells, whereas miR-200b knockdown resulted in reduced migration. Additionally, the expression of E-Cadherin was downregulated, whereas that of N-Cadherin was upregulated in miR-200b mimic-transfected cells, suggesting an increase in epithelial-mesenchymal transition. Downstream, using four target gene prediction tools, six target genes of miR-200b were predicted, amongst which, ETS proto-oncogene 1 transcription factor (*ETS1*) was shown to be significantly associated with tumor invasion depth and negatively associated with miR-200b expression. The interaction between miR-200b and *ETS1* was confirmed using a dual-luciferase reporter assay. Using rescue experiments, the increased migratory ability of the miR-200b-overexpressing cells was reversed by *ETS1* overexpression. In summary, this study showed that miR-200b overexpression serves a carcinogenic role and promotes the migration of BEAS-2B cells following long-term exposure to CS by targeting *ETS1*.

Correspondence to: Professor Jianxiang Li, Department of Toxicology, School of Public Health, Medical College of Soochow University, 199 Ren'ai Road, Industrial Park, Suzhou, Jiangsu 215123, P.R. China
E-mail: aljxcr@suda.edu.cn

*Contributed equally

Key words: cigarette smoke, microRNA-200b, migration, lung cancer

Introduction

Lung cancer is the most prevalent type of cancer in the world, accounting for ~1.8 million new lung cancer cases and 1.6 million lung cancer-associated deaths annually (1). The 5-year survival rate of patients with lung cancer varies from 4-17%, based on their pathological stage and region (2). Lung cancer can be categorized as either non-small cell lung cancer or small cell lung cancer according to its pathological features. The early symptoms of lung cancer are not obvious, usually resulting in diagnosis in the middle or later stages of its development (3). The etiological complexity and frequent metastasis of lung cancer are the primary factors underlying the difficulty in treatment and the high mortality rates associated with it (4). Tumor metastasis is a complex biological process, and its mechanism is poorly understood. The epithelial-mesenchymal transition (EMT) process is considered an early and critical step in the tumor metastatic cascade (5). Cigarette smoking is the leading cause of all histological types of lung cancer (6). Our previous work on the carcinogenic potential of cigarette smoke (CS) in normal human bronchial epithelial (BEAS-2B) cells showed aberrant DNA methylation and transcriptional profiles, as well as an increase in tumorgenicity and migratory ability (7-9).

MicroRNAs (miRNAs/miRs) are endogenous single-stranded non-coding RNAs of ~20-24 nucleotides in length (10). It has been widely reported that miRNAs negatively regulate the expression of various mRNAs by binding to the 3'-untranslated regions (3'-UTR) of mRNAs (11). miRNAs exhibit unique and diverse expression patterns and modulate several cellular processes and signaling pathways related to tumorigenesis, cell proliferation, metastasis, invasion and apoptosis (12,13). Our previous study identified multiple miRNAs that are aberrantly expressed in CS-induced malignantly transformed cells (9). The present study focused on one of these miRNAs, miR-200b, as the aberrant expression of the miR-200 family has been reported to be associated with the occurrence and development of various types of malignant tumors, such as hepatocellular carcinoma (14), colon cancer (15), breast cancer (16), ovarian cancer (17) and lung cancer (18). The miR-200 family is comprised of five members, miR-200a,

miR-200b, miR-200c, miR-429 and miR-141. Accumulating evidence suggests that miR-200b serves an important role in EMT, cancer stem cell maintenance, apoptosis and in the cell cycle (19). miR-200b has also been reported to be upregulated in lung cancer cells, where it is associated with cell proliferation and metastasis (20). However, the exact role of miR-200b in mediating lung cancer cell migration and invasion, as well as the underlying molecular mechanisms involved remain to be determined.

The aim of the present study was to identify the biological function and regulatory mechanism of miR-200b in the CS-induced malignant transformed BEAS-2B cells to explore the molecular mechanisms underlying CS-induced lung cancer. Bioinformatics analysis and *in vitro* experiments were used to analyze and verify the function and target gene of miR-200b.

Materials and methods

Data source and bioinformatics analysis. Log2 transformed RNA-seq expression data in lung cancer tissues, including lung adenocarcinoma [The Cancer Genome Atlas (TCGA) LUAD] and lung squamous cell carcinoma (TCGA LUSC), were obtained from TCGA database through the University of California Santa Cruz (UCSC) Xena Browser (xena.ucsc.edu) (21). Additionally, four datasets for the analysis of miR-200b-3p (miR-200b), accession nos. GSE62182 (22), GSE74190 (23), GSE51853 (24) and GSE48414 (25), and two datasets for ETS proto-oncogene 1 transcription factor (*ETS1*) analysis, accession nos. GSE19804 (26) and GSE27262 (27), were downloaded from the Gene Expression Omnibus (GEO) database (ncbi.nlm.nih.gov/geo/). The protein levels were determined using the 'CPTAC lung adenocarcinoma' dataset, which was downloaded from the Clinical Proteomic Tumor Analysis Consortium (CPTAC) data portal (cptac-data-portal.georgetown.edu/cptacpublic) (28). The Pearson correlation analysis of miR-200b with *ETS1* was analyzed using the webtool 'LinkedOmics' (linkedomics.org/admin.php). Enrichment analysis was performed using the webtool Database for Annotation, Visualization and Integrated Discovery (DAVID; david.ncifcrf.gov/).

Cell culture. Normal human bronchial epithelial cells (BEAS-2B), as well as lung adenocarcinoma cells (A549 and H1299) and lung squamous carcinoma cells (H226) were obtained from the American Type Culture Collection and cultured in high-glucose DMEM (Biological Industries; Sartorius AG) supplemented with 10% FBS (Biological Industries; Sartorius AG) in a 37˚C incubator with 5% CO_2.

In vitro cell model for CS-induced malignant transformation. The BEAS-2B cells were used to establish an *in vitro* model of CS-induced malignant transformation, the detailed procedure of which has been described previously (7). Briefly, aliquots of exponentially growing BEAS-2B cells ($1x10^5$) were plated onto a Transwell membrane (0.4 μm pore; Corning, Inc.). An automatic smoking machine was used to produce CS, which was then pumped into an inhalation chamber where the BEAS-2B cells were directly exposed to CS for 10 min every other day at a smoke concentration of 20%. This procedure of exposing cells to CS was continued for 10, 20 and 30 passages, and such cells were referred to as experimental S10, S20 and S30 cells, respectively. BEAS-2B cells that were not exposed to CS were used as the control cells.

Transfection. Aliquots containing $2x10^5$ BEAS-2B cells were seeded in each well of 6-well plates and cultured for 24 h. Then, the cells were transfected with: i) 50 nM mimic of miR-200b (UAAUACUGCCUGGUAAUGAUGA); ii) mimic negative control (NC, UUCUCCGAACGUGUCA); iii) 100 nM inhibitor of miR-200b (UCAUCAUUACCAGGCGGUAUUA); or iv) 5-carboxyfluorescein (FAM) labeled inhibitor NC (CAGUACUUUUGUGUAGUACAA). The four oligos were obtained from Guangzhou RiboBio Co., Ltd. Transfection was performed using Lipofectamine® 6000 reagent (Invitrogen; Thermo Fisher Scientific, Inc.) according to the manufacturer's protocol. Transfection efficiency was evaluated by reverse transcription-quantitative (RT-q)PCR and fluorescence of FAM-inhibitor NC transfected cells. The cells were harvested 24 h after transfection and used for wound healing and Transwell assays, as well as for RNA and protein extraction, as described below.

Wound healing assay. Aliquots of $2x10^5$ exponentially growing mimic- and inhibitor-transfected cells were seeded into separate 6-well plates and cultured under standard conditions until they reached 100% confluency. Subsequently, a scratch was made on each plate using a P10 pipette tip. The culture medium was replaced with fresh serum-free DMEM and the cells were cultured further. Images of the wound were obtained at 0 and 24 h using an inverted microscope (magnification, x200; Olympus Corporation) and quantitated using ImageJ version 1.8.0 (National Institutes of Health).

Transwell migration assay. Aliquots of exponentially growing transfected cells ($2x10^5$ cells in 500 μl serum-free medium) were seeded into the upper chambers of the Transwell inserts (Corning, Inc.), whereas the lower chambers were filled with 1 ml complete medium with 10% FBS. All plates were incubated at 37˚C for 24 h. Subsequently, the cells on the membrane of the upper chamber were removed with a cotton swab. Cells in the lower chamber were fixed with 4% paraformaldehyde at room temperature for 15 min and stained with 0.5% crystal violet solution at room temperature for 15 min. Images of the cells were taken using an inverted microscope (magnification, x200; Olympus Corporation) and analyzed using ImageJ version 1.8.0 (National Institutes of Health).

RNA extraction and RT-qPCR. Total RNA was extracted using TRIzol® reagent (Thermo Fisher Scientific, Inc.) according to the manufacturer's instructions from cell samples. From each sample, ~1.5 μg RNA was reverse transcribed into cDNA using a RevertAid First Strand cDNA Synthesis Kit for mRNA detection (Thermo Fisher Scientific, Inc.), or a Mir-X™ miRNA First-Strand Synthesis kit for miRNA detection (Clontech Laboratories, Inc.) according to the manufacturer's instructions. qPCR was performed using a NovoScript® SYBR Two-Step RT-qPCR kit (Novoprotein Scientific, Inc.) on a QuantStudio™ 6 Flex RT-qPCR system (Applied Biosystems; Thermo Fisher Scientific, Inc.). Thermocycling conditions were initial hold at 95˚C for 10 min, 40 cycles of 95˚C for

15 sec and 60˚C for 60 sec. The sequences of the primer pairs used for qPCR are listed in Table SI. GAPDH and U6 were used as the internal controls. The relative expression of each target was analyzed using the $2^{-\Delta\Delta Cq}$ method (29).

Protein extraction and western blot analysis. Exponentially growing cells were washed with ice-cold PBS and lysed in ice-cold RIPA buffer (Beyotime Institute of Biotechnology) for protein extraction. Total protein was quantified using BCA reagent (Beyotime Institute of Biotechnology). Then, ~30 μg of each protein sample was mixed with a quarter volume of 5X loading buffer and boiled at 95˚C for 10 min. The lysates were loaded on a 10% sodium dodecyl sulfate (SDS)-gel, resolved using SDS-polyacrylamide gel electrophoresis, and subsequently the proteins were transferred to PVDF membranes (EMD Millipore). The membranes were blocked using TBS with 0.1% Tween-20 (TBST) buffer containing 5% BSA (Beyotime Institute of Biotechnology) at room temperature for 2 h, and then probed with specific primary antibodies overnight at 4˚C. After washing with TBST, membranes were incubated at room temperature for 2 h with mouse or rabbit anti-rabbit IgG antibody. The antibodies used in this experiment were: Epithelial marker, E-cadherin (CDH1; 1:1,000; cat. no. 20874-1-AP; ProteinTech Group, Inc.), mesenchymal marker, N-cadherin (CDH2; 1:1,000; cat. no. 22018-1-AP; ProteinTech Group, Inc.), GAPDH (1:1,000; cat. no. 5174; Cell Signaling Technology, Inc.), horseradish peroxidase (HRP)-conjugated anti-rabbit IgG secondary antibody (1:20,000; cat. no. ab7090; Abcam) and HRP-tagged anti-mouse IgG secondary antibody (1:3,000; cat. no. 7076; Cell Signaling Technology, Inc.). Signals were visualized using enhanced chemiluminescence (ECL) plus reagents (Invitrogen; Thermo Fisher Scientific, Inc.) and a GeneTools GBox system (Syngene Europe). The intensity of each band was semi-quantified using ImageJ.

Dual-luciferase reporter assays. To verify whether *ETS1* was a direct target of miR-200b, the complete sequence of the *ETS1* wild-type 3'-UTR (ETS1_UTR_WT) was amplified by PCR from human genomic DNA using the forward primer, 5'-GCTCTAGAGCTATCACTCTAGTTTTGAAGC-3' and reverse primer, 5'-GCTCTAGAGCCTTTCATTGTGACAGAA TCC-3'. Both primers contained the recognition sequence for the *Xba*I restriction enzyme at the 5' ends. Subsequently, the sequence was cloned into the pGL3 (cat. no. 48743; Addgene) vector downstream of the luciferase open reading frame. Additionally, the site-directed mutagenesis for *ETS1* 3'-UTR was performed using a site-directed mutagenesis kit (Beyotime Institute of Biotechnology) to remove the miR-200b binding site.

Aliquots of $2x10^5$ exponentially growing BEAS-2B cells were seeded into 24-well plates and co-transfected with the mimics (miR-200b) and the constructed pGL3 plasmids, as well as the Renilla luciferase plasmid (pRL, Addgene, cat. no. 27163, which was used as the internal control) at a ratio of 5:5:1 using Lipofectamine® 2000 (Invitrogen; Thermo Fisher Scientific, Inc.). Lysates were collected 48 h after transfection. Firefly and *Renilla* luciferase activities were measured using a Firefly luciferase Reporter Gene Assay kit (Beyotime Institute of Biotechnology).

Target gene prediction. The target genes of miRNAs were predicted using miRDB (mirdb.org/miRDB/), miRTarBase (mirtarbase.cuhk.edu.cn/php/index.php) and miRanda (microrna.org/) online analysis tools. To further enhance the reliability of bioinformatics analysis, the overlapping target genes were identified using a Venn diagram generated with VennDiagram package (version: 1.6.20) in R (version: 4.0.4).

ETS1 plasmid construction and rescue testing. The complete coding sequence of *ETS1* was amplified by PCR from human genomic DNA using the forward primer, 5'- GGAATTCC GCCACCATGAGCTACTTTGTGGATTCT-3' and reverse primer, 5'- ACGCGTCGACTCACTCGTCGGCATCTGG CTT-3'. The *ETS1* plasmid was constructed by inserting the CDS into a mammalian expression vector, pCDH-EF1-copGFP (Addgene, Inc.), which contained a CMV promoter driving the expression of GFP and ETS1. The negative control used in this study was the empty vector. A total of 2.5 μg pCDH-EF1-copGFP-ETS1 (pCDH ETS1) or empty vector (pCDH Blank) was transfected into BEAS-2B cells (10^5 cells per well of 6-well plate) to rescue the low-expression induced by mimic transfection. Transfection was performed using Lipofectamine® 6000 reagent (Invitrogen; Thermo Fisher Scientific, Inc.) according to the manufacturer's protocol. After 48 h, transfected cells were harvested for further detection.

Statistical analysis. All results are presented as the mean ± standard deviation (n=3 replicates for each experiment) and were analyzed using SPSS version 22.0 (IBM Corp.). Histograms were plotted using GraphPad Prism version 7 (GraphPad Software, Inc.). Differences between groups were compared using an unpaired Student's t-test or a one-way ANOVA with a Tukey's post hoc test where appropriate. $P<0.05$ was considered to indicate a statistically significant difference.

Results

miR-200b expression is upregulated in CS-exposed cells and lung cancer cell lines. Our previous study identified several differentially expressed miRNAs, including miR-200b-3p (miR-200b), based on the miRNA sequencing results (8) (Fig. 1A). The results from RT-qPCR analysis indicated that miR-200b was significantly upregulated in S10, S20 and S30 cells (Fig. 1B), as well as in human lung cancer cells, including A549, H1299 and H226 (Fig. 1C). Next, the expression of miR-200b in six lung cancer datasets was analyzed. The results showed that miR-200b was significantly increased in lung cancer tissues when compared with normal tissues (Fig. 1D-I).

miR-200b promotes migration of lung cancer cells. Using the LinkedOmics online tool, positively and negatively correlated genes of miR-200b-5p in LUAD and LUSC were obtained (Fig. S1A and B). A total of 380 and 818 overlapping genes were significantly positively and negatively correlated with miR-200b in both LUAD and LUSC datasets, respectively (Fig. S1C and D). Additionally, further enrichment analysis demonstrated that these correlated genes were significantly enriched in several cancer-related signaling pathways, particularly cell migration-related pathways, including 'Focal adhesion', 'ECM-receptor interaction', 'Cell adhesion molecules' and 'NF-kappa B' and 'Jak-STAT' signaling

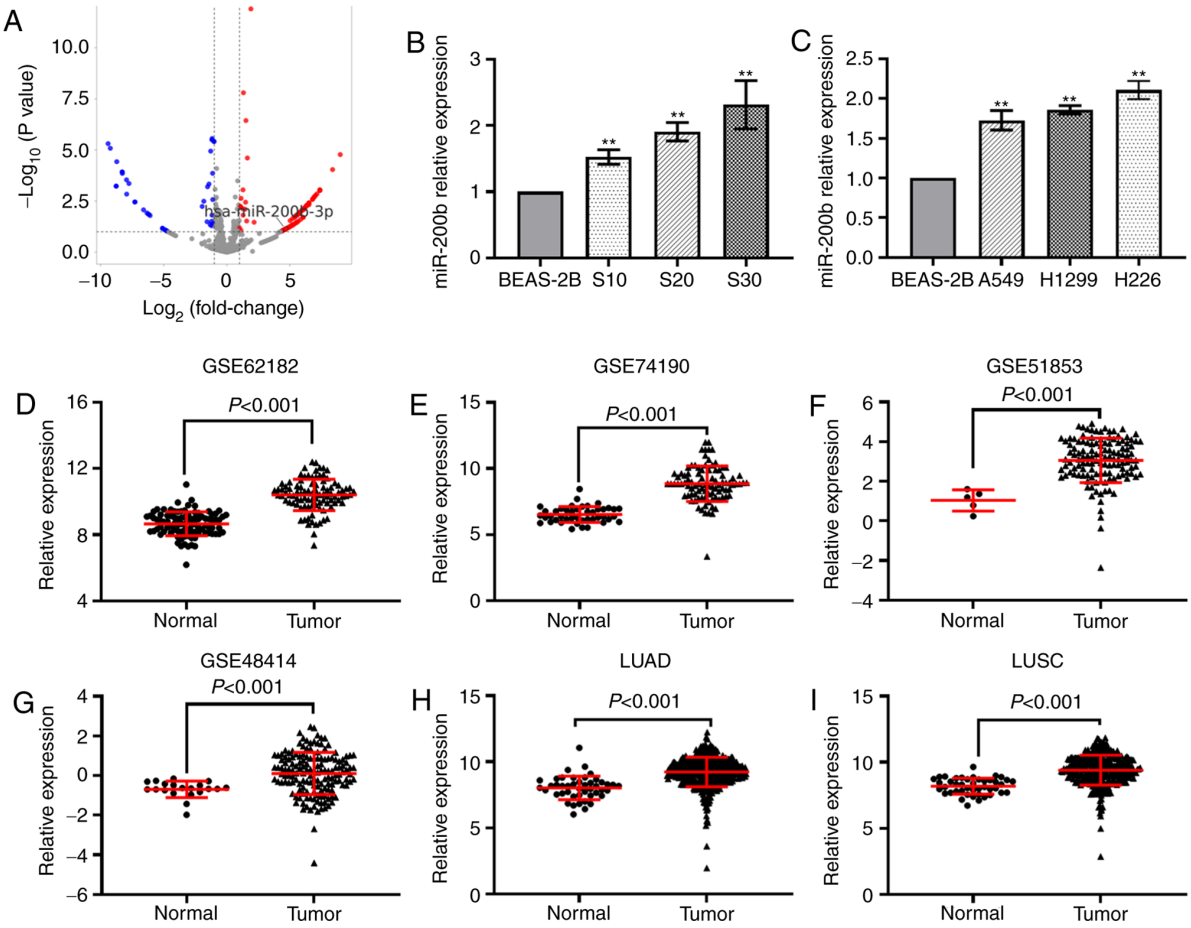

Figure 1. miR-200b is upregulated in CS-exposed cells and lung cancer. (A) Reverse transcription-quantitative PCR analysis of miR-200b in (B) CS-exposed BEAS-2B cells and (C) lung cancer cells. Differential analysis of miR-200b expression in six datasets, (D) GSE62182, (E) GSE74190, (F) GSE51853, (G) GSE48414, as well as in the (H) LUAD and (I) LUSC datasets in The Cancer Genome Atlas. **P<0.01 vs. normal BEAS-2B cells. miR, microRNA; CS, cigarette smoke; qPCR, quantitative PCR; LUAD, lung adenocarcinoma; LUSC, lung squamous cell carcinoma.

pathways (Fig. S1E). Transfection efficiency was evaluated by RT-qPCR and FAM-inhibitor NC. RT-qPCR results revealed that miR-200b-5p levels were elevated significantly in the mimic-transfected cells, compared with mimic NC-transfected cells (Fig. S2A). Fluorescent imaging demonstrated that the FAM-inhibitor NC became abundant within the cells, suggesting that the miRNA oligos used in this study were successfully transfected into BEAS-2B cells s(Fig. S2B). The results from the Transwell and wound-healing assays showed that transfection of cells with miR-200b mimic enhanced the migration of BEAS-2B cells. Conversely, transfection with the inhibitor of miR-200b significantly reduced the migratory capability of BEAS-2B cells (Fig. 2A-D). The results also showed that the mRNA expression levels of CDH1 were downregulated in cells transfected with miR-200b mimic, whereas they were upregulated in cells transfected with the miR-200b inhibitor (Fig. 2E). By contrast, CDH2 mRNA expression was upregulated in cells transfected with miR-200b mimic and downregulated in cells transfected with miR-200b inhibitors (Fig. 2F). The changes in protein levels of CDH1 and CDH2 in the transfected cells were consistent with the changes in mRNA expression (Fig. 2G-I).

ETS1 is a target of miR-200b in lung cancer cells. Using the TargetScan, miRanda, miRWalk and miRTarBase online tools, a total of six intersected target genes of miR-200b were obtained, including *ETS1*, *ZFPM2*, *RND3*, *E2F3*, *QKI* and *XIAP* (Fig. 3A). The pathological analysis indicated that in TCGA LUAD dataset, *ETS1* expression was downregulated in lung cancer tissues at advanced invasion depth (T2) compared with tissues at stage T1 (Fig. 3B). The decreased expression of *ETS1* in lung cancer tissues of patients was found in TCGA LUAD (Fig. 3C), TCGA LUSC (Fig. 3D), GSE19804 (Fig. 3E), and GSE27262 (Fig. 3F) datasets, as well as in the proteomics dataset, CPTAC_LUAD (Fig. 3G). Additionally, the RT-qPCR and western blot analysis showed significant downregulation of *ETS1* in S20 and S30 cells (Fig. 3H and I).

In addition, correlation analysis revealed that the expression levels of miR-200b were weakly and moderately negatively correlated with *ETS1* mRNA expression in TCGA LUAD (Fig. 4A) and TCGA LUSC (Fig. 4B) datasets respectively. The mRNA and protein expression levels of *ETS1* were significantly downregulated in cells transfected with miR-200b mimics, whereas expression was upregulated in cells transfected with inhibitors (Fig. 4C and D). As shown in Fig. 4E, two binding sites for miR-200b were present in the 3'UTR of *ETS1*. The relative luciferase activity of the reporter gene in BEAS-2B cells co-transfected with pGL3-ETS1 WT 3'UTR and miR-200b mimic was significantly decreased compared with the control (co-transfected with pGL3-ETS1 3'UTR and

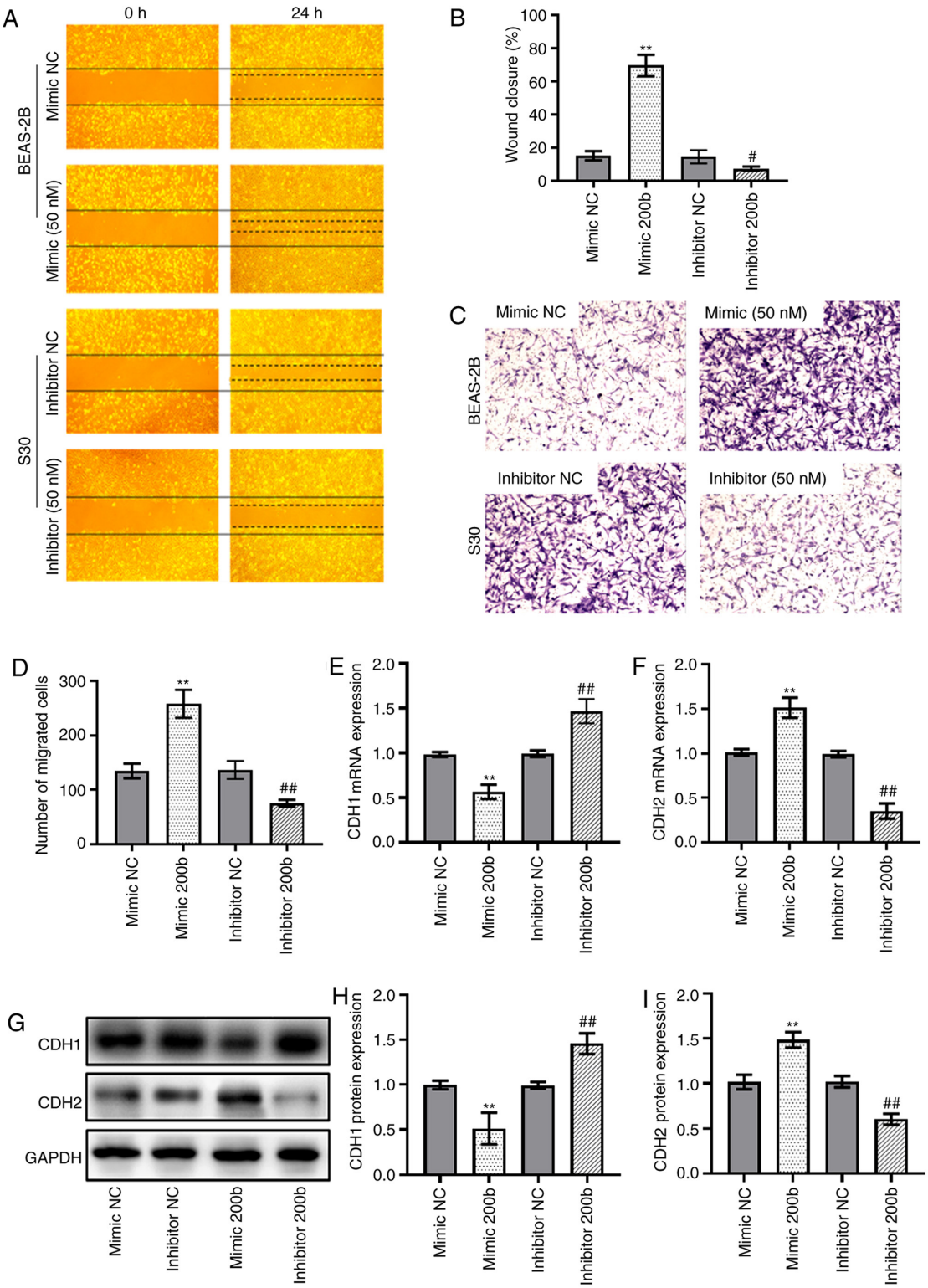

Figure 2. miR-200b promotes BEAS-2B cell migration. (A) Representative images and (B) quantification of wound healing assays showing cell migration was significantly increased in mimic-transfected BEAS-2B cells. (C) Representative images and (D) quantification of Transwell migration assays of BEAS-2B cells transfected with miR-200b mimics or inhibitors. Reverse transcription-quantitative PCR analysis of (E) *CDH1* and (F) *CDH2* expression in BEAS-2B cells transfected with mimics or inhibitors. (G) Western blot analysis of CDH1 and CDH2 in BEAS-2B cells transfected with mimics or inhibitors. Semi-quantitative results of the protein expression levels of (H) CDH1 and (I) CDH2 in BEAS-2B cells transfected with mimics or inhibitors. **P<0.01 vs. mimic NC group; $^{\#}$P<0.05, $^{\#\#}$P<0.01 vs. inhibitor NC group. miR, microRNA; NC, negative control; CDH1, E-Cadherin; CDH2, N-Cadherin.

mimic NC). Mutating one of the two binding sites alone can still result in downregulation of relative luciferase activity when compared with mimic NC groups, whereas mutating both sites simultaneously avoids this downregulation (Fig. 4F).

ETS1 mediates the pro-migration effect of miR-200b. To further confirm that the effects of miR-200b were mediated by repression of *ETS1* in BEAS-2B cells, rescue experiments in which ETS1 was overexpressed were performed. The transfection

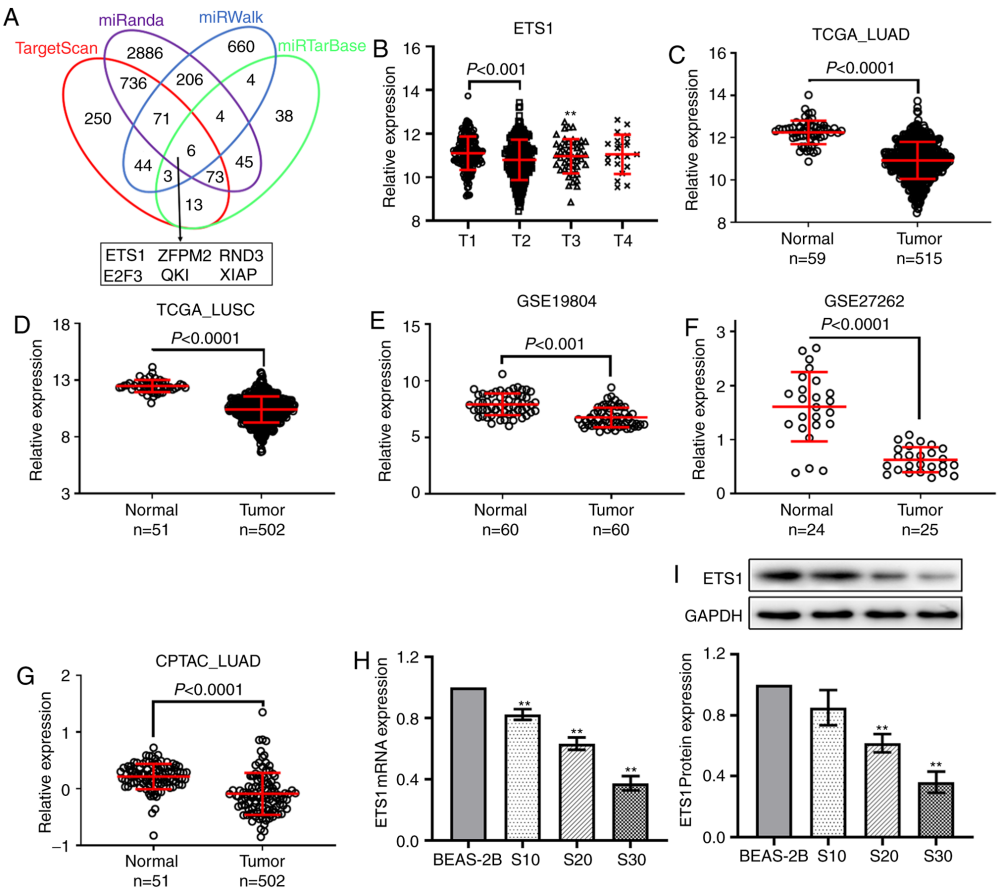

Figure 3. ETS1 is a downstream target of miR-200b. (A) Venn diagram showing the intersection of the target genes predicted by four online tools, TargetScan, miRanda, miRWalk and miRTarBase. (B) In TCGA LUAD dataset, *ETS1* was downregulated in lung cancer tissues at stage T2 compared with tissues at stage T1. Differential analysis of *ETS1* expression in four datasets, (C) TCGA LUAD, (D) TCGA LUSC, (E) GSE19804 and (F) GSE27262, as well as the (G) CPTAC LUAD proteomics dataset. (H) Reverse transcription-quantitative PCR analysis showed *ETS1* expression was downregulated in CS-exposed cells. (I) Western blotting results showed ETS1 protein expression was downregulated in CS-exposed cells. **P<0.01 vs. normal BEAS-2B cells. TCGA, The Cancer Gene Atlas; CPTAC, Clinical Proteomic Tumor Analysis Consortium; LUAD, lung adenocarcinoma; LUSC, lung squamous cell carcinoma; CS, cigarette smoke; miR, microRNA; ETS1, ETS proto-oncogene 1 transcription factor; ZFPM2, zinc finger protein ZFPM2; RND3, rho-related GTP-binding protein RhoE; E2F3, transcription factor E2F3; QKI, protein quaking; XIAP, E3 ubiquitin-protein ligase XIAP.

efficiency of ETS1 overexpression vectors was verified by RT-qPCR (Fig. S2C) and western blot (Fig. S2D and E). The enhanced migratory ability of BEAS-2B cells induced by miR-200b mimic was reduced by transfection of the ETS1 overexpression vector. Compared with the cells transfected with mimic NC and blank vector, BEAS-2B cells transfected with miR-200b mimic and blank vector exhibited increased migration ability. However, the enhanced migratory ability induced by the mimic miR-200b was downregulated by co-transfection with the ETS1 vector (Fig. 5A and B). In the wound healing assays, a similar trend was observed (Fig. 5C and D).

Discussion

Previously, it has been reported that certain miRNAs directly activate EMT transcription factors, whereas others are able to reverse the EMT process by targeting several signaling pathways (10). In the present study, miR-200b was demonstrated to be involved in the migration and EMT process of lung cancer cells. miR-200b is a member of the miR-200 family and has been reported to serve contrasting roles in different types of cancer. Studies reported that its expression is downregulated in several malignant tumors, exhibiting a tumor-suppressing role (30-33). For example, miR-200b was identified as a repressor of invasiveness in esophageal squamous cell carcinoma by modulating multiple key cell cycle regulators and the Wnt/β-catenin signaling pathways (34). Conversely, miR-200b has also been found to promote cellular proliferation and serve a tumor-promoting role in several other tumors, such as cervical cancer and colorectal cancer, as well as in lung cancer (20,35-37). It has been reported that miRNA dysregulation may serve as a biomarker of damage caused by acute and chronic environmental exposure (38). Our previous miRNA high throughput sequencing analysis identified several differentially expressed miRNAs in the CS-induced malignantly transformed BEAS-2B cells (9). In the present study, elevated miR-200b levels were found in the CS-induced malignant BEAS-2B cells and several lung cancer cell lines, which was corroborated by analysis of external lung cancer tissue databases. Furthermore, it was demonstrated that miR-200b overexpression significantly enhanced the cellular migratory ability and EMT of cells as demonstrated by the reduction in CDH1 expression and increase in CDH2 expression levels. Importantly, these alterations in cell behavior have also been demonstrated in CS-induced malignantly transformed cells (9).

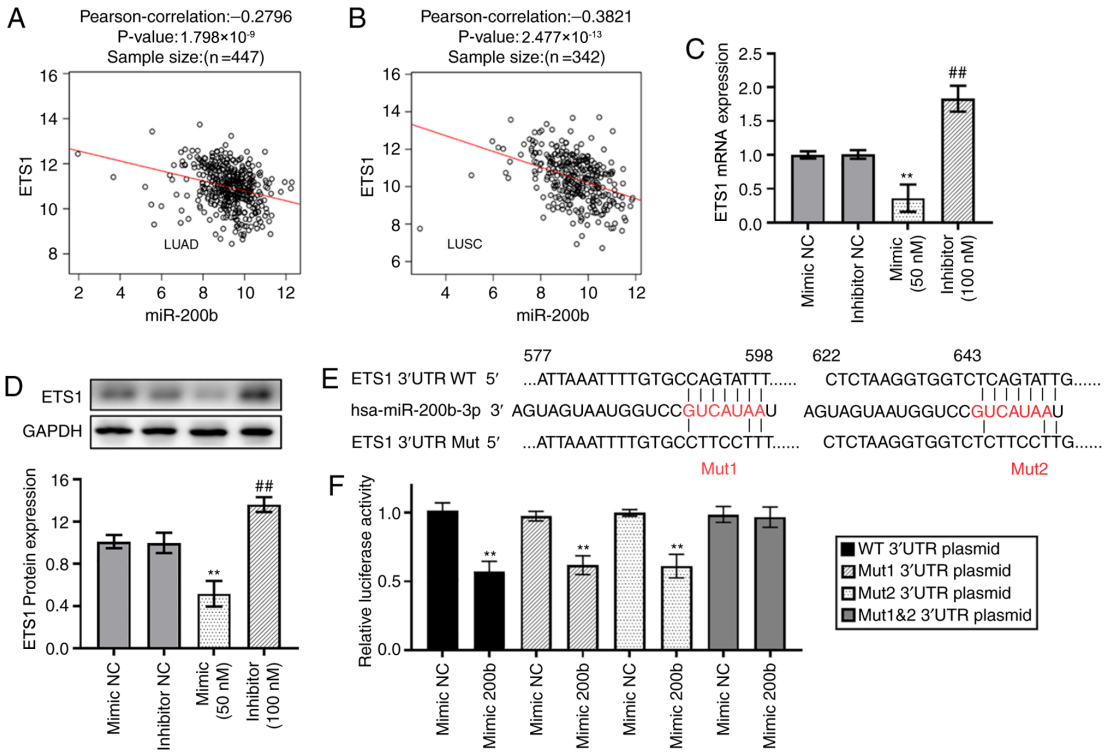

Figure 4. *ETS1* is directly regulated by miR-200b. Correlation between *ETS1* and miR-200b expression levels in (A) TCGA LUAD and (B) TCGA LUSC datasets. (C) *ETS1* mRNA expression levels in the mimic- or inhibitor-transfected BEAS-2B cells. (D) Western blotting results of ETS1 expression in the mimic- or inhibitor-transfected BEAS-2B cells. (E) Sequence comparison between miR-200b-3p and the 3'UTR of ETS1. (F) Relative luciferase activity was measured in BEAS-2B cells co-transfected with 50 nM miR-200b mimic and the pGL3-ETS1 3'UTR construct. **P<0.01 vs. mimic NC group; $^{\#\#}$P<0.01 vs. inhibitor NC group. TCGA, The Cancer Gene Atlas; LUAD, lung adenocarcinoma; LUSC, lung squamous cell carcinoma; UTR, untranslated region; miR, microRNA; ETS1, ETS proto-oncogene 1 transcription factor; NC, negative control; WT, wild-type; Mut, mutant.

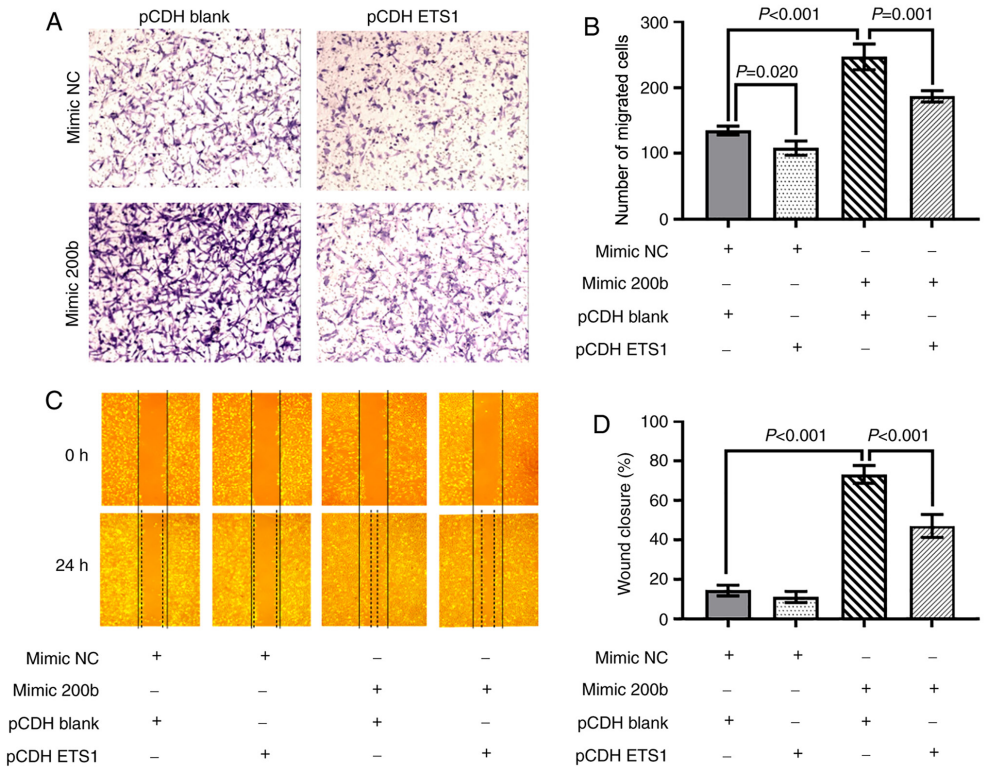

Figure 5. Overexpression of ETS1 reverses the pro-migratory effect of miR-200b upregulation. (A) Representative images and (B) quantification of the Transwell migration assays of BEAS-2B cells co-transfected with miR-200b mimic and an ETS1 overexpression vector. (C) Representative images and (D) quantification of wound healing assays showing significant increases in cell migration in the miR-200b mimic-transfected BEAS-2B cells, which was partially reversed following ETS1 overexpression. pCDH Blank, empty pCDH-EF1-copGFP vector; pCDH ETS1, ETS1 overexpression plasmid constructed from pCDH-EF1-copGFP; miR, microRNA; ETS1, ETS proto-oncogene 1 transcription factor; NC, negative control.

ETS1 is a 54-kDa nuclear protein that serves a major role in the regulation of transcription factors (39). Transcription factors of the ETS family are involved in normal cell development, proliferation and differentiation (40). Previously, studies have found multiple miRNAs that downregulate ETS1 expression by directly targeting the 3'UTR region of *ETS1* (41). For example, in human hepatocellular carcinoma cells, miR-1, miR-129-5p, miR-193b and miR-499 can induce the downregulation of ETS1 expression, and thus reduce migration and invasion (42-44).

Similar to a previous study (45), it was presented in the present study that *ETS1* was a target gene of miR-200b, through multiple target gene prediction databases. The dual-luciferase reporter assay confirmed this targeting regulatory relationship between miR-200b and *ETS1*. However, multiple aspects distinguish the present study from previously published literature. In the present study, not only did we show the downregulation of *ETS1* expression in lung cancer cell lines *in vitro* and in tumor tissue samples, but we also further confirmed this relationship using a controlled model of long-term CS-exposed cells. Moreover, in addition to establishing the importance of the miR-200b-ETS1 cascade in elevating the migratory ability of cells, we further showed a reversal of the miR-200b-induced increase in migration when ETS1 overexpression plasmids were transfected into the miR-200b overexpressing BEAS-2B cells. Similarly, this increase in migratory ability was dampened by transfection of miR-200b inhibitors.

The present study had some limitations that are worth mentioning. First, only one cell line, the immortalized bronchial epithelial cell BEAS-2B, was used to investigate the role of miR-200b in promoting migration, while no lung cancer cell lines were used for comparative analysis. The present study also lacks the necessary animal experiments for miR-200b function. Further studies will shed more light on its function with more *in vitro* or *in vivo* experiments.

In summary, the present study demonstrated the upregulation of miR-200b in CS-exposed BEAS-2B cells, lung cancer cell lines and tumor tissue samples. Downstream, miR-200b was shown to serve a carcinogenic role by targeting the 3'-UTR of *ETS1*, in-turn promoting cell migration and EMT. These insights into the miR-200b-*ETS1* axis may facilitate the development of treatments for CS-induced lung cancer. With the development of improved delivery vehicles for these therapeutics, we hypothesize that miRNA therapies will soon become a clinical reality in the treatment of cancer.

Acknowledgements

Not applicable.

Funding

This study was supported by the National Natural Science Foundation of China (grant no. 81573178), Jiangsu Key Laboratory of Preventive and Translational Medicine for Geriatric Diseases, the Priority Academic Program Development of Jiangsu Higher Education Institutions (PAPD) and Postgraduate Research & Practice Innovation Program of Jiangsu Province (grant no. KYCX20_2681).

Availability of data and materials

The TCGA LUAD and LUSC datasets analyzed during the current study are available in the UCSC Xena repository, [https://xenabrowser.net/datapages/]. The datasets analyzed during the current study are available in the GEO repository, [https://ncbi.nlm.nih.gov/geo/].

Authors' contributions

JL and JW conceived and designed the study. RY, JW and YL retrieved and downloaded the datasets. JW, RY, QL and YL analyzed the datasets. RY, QL, LT, JT, BJ and NO performed the experiments and analyzed the data. JL and JW confirm the authenticity of all the raw data. JW and RY drafted the manuscript. QL, JL, YL and JT edited the manuscript. All authors have read and approved the final manuscript.

Ethics approval and consent to participate

Not applicable.

Patient consent for publication

Not applicable.

Competing interests

The authors declare that they have no competing interests.

References

1. Ferlay J, Soerjomataram I, Dikshit R, Eser S, Mathers C, Rebelo M, Parkin DM, Forman D and Bray F: Cancer incidence and mortality worldwide: Sources, methods and major patterns in GLOBOCAN 2012. Int J Cancer 136: E359-E386, 2015.
2. Hirsch FR, Scagliotti GV, Mulshine JL, Kwon R, Curran WJ Jr, Wu YL and Paz-Ares L: Lung cancer: Current therapies and new targeted treatments. Lancet 389: 299-311, 2017.
3. Goebel C, Louden CL, McKenna R Jr, Onugha O, Wachtel A and Long T: Diagnosis of non-small cell lung cancer for early stage asymptomatic patients. Cancer Genomics Proteomics 16: 229-244, 2019.
4. Hay ED: An overview of epithelio-mesenchymal transformation. Acta Anat (Basel) 154: 8-20, 1995.
5. Kalluri R and Weinberg RA: The basics of epithelial-mesenchymal transition. J Clin Invest 119: 1420-1428, 2009.
6. Lamouille S, Xu J and Derynck R: Molecular mechanisms of epithelial-mesenchymal transition. Nat Rev Mol Cell Biol 15: 178-196, 2014.
7. Du H, Sun J, Chen Z, Nie J, Tong J and Li J: Cigarette smoke-induced failure of apoptosis resulting in enhanced neoplastic transformation in human bronchial epithelial cells. J Toxicol Environ Health A 75: 707-720, 2012.
8. Huang H, Ji Y, Zhang J, Su Z, Liu M, Tong J, Ge C, Chen T and Li J: Aberrant DNA methylation in radon and/or cigarette smoke-induced malignant transformation in BEAS-2B human lung cell line. J Toxicol Environ Health A 80: 1321-1330, 2017.
9. Wang J, Yu XF, Ouyang N, Zhao S, Yao H, Guan X, Tong J, Chen T and Li JX: MicroRNA and mRNA Interaction network regulates the malignant transformation of human bronchial epithelial cells induced by Cigarette smoke. Front Oncol 9: 1029, 2019.
10. Zaravinos A: The regulatory role of MicroRNAs in EMT and cancer. J Oncol 2015: 865816, 2015.
11. Gros J and Tabin CJ: Vertebrate limb bud formation is initiated by localized epithelial-to-mesenchymal transition. Science 343: 1253-1256, 2014.

12. Correa-Costa M, Andrade-Oliveira V, Braga TT, Castoldi A, Aguiar CF, Origassa CS, Rodas AC, Hiyane MI, Malheiros DM, Rios FJ, *et al*: Activation of platelet-activating factor receptor exacerbates renal inflammation and promotes fibrosis. Lab Invest 94: 455-466, 2014.
13. Grande MT, Sánchez-Laorden B, López-Blau C, De Frutos CA, Boutet A, Arévalo M, Rowe RG, Weiss SJ, López-Novoa JM and Nieto MA: Snail1-induced partial epithelial-to-mesenchymal transition drives renal fibrosis in mice and can be targeted to reverse established disease. Nat Med 21: 989-997, 2015.
14. Dhayat SA, Mardin WA, Köhler G, Bahde R, Vowinkel T, Wolters H, Senninger N, Haier J and Mees ST: The microRNA-200 family - a potential diagnostic marker in hepatocellular carcinoma? J Surg Oncol 110: 430-438, 2014.
15. Hur K, Toiyama Y, Takahashi M, Balaguer F, Nagasaka T, Koike J, Hemmi H, Koi M, Boland CR and Goel A: MicroRNA-200c modulates epithelial-to-mesenchymal transition (EMT) in human colorectal cancer metastasis. Gut 62: 1315-1326, 2013.
16. Bojmar L, Karlsson E, Ellegård S, Olsson H, Björnsson B, Hallböök O, Larsson M, Stål O and Sandström P: The role of microRNA-200 in progression of human colorectal and breast cancer. PLoS One 8: e84815, 2013.
17. Kan CW, Hahn MA, Gard GB, Maidens J, Huh JY, Marsh DJ and Howell VM: Elevated levels of circulating microRNA-200 family members correlate with serous epithelial ovarian cancer. BMC Cancer 12: 627, 2012.
18. Pacurari M, Addison JB, Bondalapati N, Wan YW, Luo D, Qian Y, Castranova V, Ivanov AV and Guo NL: The microRNA-200 family targets multiple non-small cell lung cancer prognostic markers in H1299 cells and BEAS-2B cells. Int J Oncol 43: 548-560, 2013.
19. Feng B, Wang R and Chen LB: Review of miR-200b and cancer chemosensitivity. Biomed Pharmacother 66: 397-402, 2012.
20. Liu K, Zhang W, Tan J, Ma J and Zhao J: miR-200b-3p functions as an oncogene by targeting ABCA1 in lung adenocarcinoma. Technol Cancer Res Treat 18: 1533033819892590, 2019.
21. Goldman MJ, Craft B, Hastie M, Repečka K, McDade F, Kamath A, Banerjee A, Luo Y, Rogers D, Brooks AN, *et al*: Visualizing and interpreting cancer genomics data via the Xena platform. Nat Biotechnol 38: 675-678, 2020.
22. Vucic EA, Thu KL, Pikor LA, Enfield KS, Yee J, English JC, MacAulay CE, Lam S, Jurisica I and Lam WL: Smoking status impacts microRNA mediated prognosis and lung adenocarcinoma biology. BMC Cancer 14: 778, 2014.
23. Huang W, Jin Y, Yuan Y, Bai C, Wu Y, Zhu H and Lu S: Validation and target gene screening of hsa-miR-205 in lung squamous cell carcinoma. Chin Med J (Engl) 127: 272-278, 2014.
24. Arima C, Kajino T, Tamada Y, Imoto S, Shimada Y, Nakatochi M, Suzuki M, Isomura H, Yatabe Y, Yamaguchi T, *et al*: Lung adenocarcinoma subtypes definable by lung development-related miRNA expression profiles in association with clinicopathologic features. Carcinogenesis 35: 2224-2231, 2014.
25. Bjaanaes MM, Halvorsen AR, Solberg S, Jørgensen L, Dragani TA, Galvan A, Colombo F, Anderlini M, Pastorino U, Kure E, *et al*: Unique microRNA-profiles in EGFR-mutated lung adenocarcinomas. Int J Cancer 135: 1812-1821, 2014.
26. Lu TP, Tsai MH, Lee JM, Hsu CP, Chen PC, Lin CW, Shih JY, Yang PC, Hsiao CK, Lai LC, *et al*: Identification of a novel biomarker, SEMA5A, for non-small cell lung carcinoma in nonsmoking women. Cancer Epidemiol Biomarkers Prev 19: 2590-2597, 2010.
27. Wei TY, Juan CC, Hisa JY, Su LJ, Lee YC, Chou HY, Chen JM, Wu YC, Chiu SC, Hsu CP, *et al*: Protein arginine methyltransferase 5 is a potential oncoprotein that upregulates G1 cyclins/cyclin-dependent kinases and the phosphoinositide 3-kinase/AKT signaling cascade. Cancer Sci 103: 1640-1650, 2012.
28. Whiteaker JR, Halusa GN, Hoofnagle AN, Sharma V, MacLean B, Yan P, Wrobel JA, Kennedy J, Mani DR, Zimmerman LJ, *et al*; Clinical proteomic tumor analysis consortium (CPTAC): CPTAC assay portal: A repository of targeted proteomic assays. Nat Methods 11: 703-704, 2014.
29. Livak KJ and Schmittgen TD: Analysis of relative gene expression data using real-time quantitative PCR and the 2(-Delta Delta C(T)) method. Methods 25: 402-408, 2001.
30. Yao Y, Hu J, Shen Z, Yao R, Liu S, Li Y, Cong H, Wang X, Qiu W and Yue L: MiR-200b expression in breast cancer: A prognostic marker and act on cell proliferation and apoptosis by targeting Sp1. J Cell Mol Med 19: 760-769, 2015.
31. Shinozaki A, Sakatani T, Ushiku T, Hino R, Isogai M, Ishikawa S, Uozaki H, Takada K and Fukayama M: Downregulation of microRNA-200 in EBV-associated gastric carcinoma. Cancer Res 70: 4719-4727, 2010.
32. He M, Liu Y, Deng X, Qi S, Sun X, Liu G, Liu Y, Liu Y and Zhao M: Down-regulation of miR-200b-3p by low p73 contributes to the androgen-independence of prostate cancer cells. Prostate 73: 1048-1056, 2013.
33. Li Y, Guan B, Liu J, Zhang Z, He S, Zhan Y, Su B, Han H, Zhang X, Wang B, *et al*: MicroRNA-200b is downregulated and suppresses metastasis by targeting LAMA4 in renal cell carcinoma. EBioMedicine 44: 439-451, 2019.
34. Zhang HF, Alshareef A, Wu C, Jiao JW, Sorensen PH, Lai R, Xu LY and Li EM: miR-200b induces cell cycle arrest and represses cell growth in esophageal squamous cell carcinoma. Carcinogenesis 37: 858-869, 2016.
35. Zhang Z, Xing T, Chen Y and Xiao J: Exosome-mediated miR-200b promotes colorectal cancer proliferation upon TGF-β1 exposure. Biomed Pharmacother 106: 1135-1143, 2018.
36. Zeng F, Xue M, Xiao T, Li Y, Xiao S, Jiang B, Ren C: MiR-200b promotes the cell proliferation and metastasis of cervical cancer by inhibiting FOXG1. Biomed Pharmacother 79: 294-301, 2016.
37. Fu Y, Liu X, Zhou N, Du L, Sun Y, Zhang X and Ge Y: MicroRNA-200b stimulates tumour growth in TGFBR2-null colorectal cancers by negatively regulating p27/kip1. J Cell Physiol 229: 772-782, 2014.
38. Vrijens K, Bollati V and Nawrot TS: MicroRNAs as potential signatures of environmental exposure or effect: A systematic review. Environ Health Perspect 123: 399-411, 2015.
39. Wang C, Kam RKT, Shi W, Xia Y, Chen X, Cao Y, Sun J, Du Y, Lu G, Chen Z, *et al*: The proto-oncogene transcription factor Ets1 regulates neural crest development through histone deacetylase 1 to mediate output of bone morphogenetic protein signaling. J Biol Chem 290: 21925-21938, 2015.
40. Shaikhibrahim Z and Wernert N: ETS transcription factors and prostate cancer: The role of the family prototype ETS-1 (Review). Int J Oncol 40: 1748-1754, 2012.
41. Dittmer J: The role of the transcription factor Ets1 in carcinoma. Semin Cancer Biol 35: 20-38, 2015.
42. Xu C, Liu S, Fu H, Li S, Tie Y, Zhu J, Xing R, Jin Y, Sun Z and Zheng X: MicroRNA-193b regulates proliferation, migration and invasion in human hepatocellular carcinoma cells. Eur J Cancer 46: 2828-2836, 2010.
43. Wei W, Hu Z, Fu H, Tie Y, Zhang H, Wu Y and Zheng X: MicroRNA-1 and microRNA-499 downregulate the expression of the ets1 proto-oncogene in HepG2 cells. Oncol Rep 28: 701-706, 2012.
44. Ma N, Chen F, Shen SL, Chen W, Chen LZ, Su Q, Zhang LJ, Bi J, Zeng WT, Li W, *et al*: MicroRNA-129-5p inhibits hepatocellular carcinoma cell metastasis and invasion via targeting ETS1. Biochem Biophys Res Commun 461: 618-623, 2015.
45. Chan YC, Khanna S, Roy S and Sen CK: miR-200b targets Ets-1 and is down-regulated by hypoxia to induce angiogenic response of endothelial cells. J Biol Chem 286: 2047-2056, 2011.